Accepted Manuscript

Design, synthesis, and evaluation of curcumin derivatives as Nrf2 activators and cytoprotectors against oxidative death

Zhi-Shan Tu, Qi Wang, Dan-Dan Sun, Fang Dai, Bo Zhou

PII: S0223-5234(17)30263-5

DOI: 10.1016/j.ejmech.2017.04.008

Reference: EJMECH 9355

To appear in: *European Journal of Medicinal Chemistry*

Received Date: 15 January 2017

Revised Date: 1 April 2017

Accepted Date: 4 April 2017

Please cite this article as: Z.-S. Tu, Q. Wang, D.-D. Sun, F. Dai, B. Zhou, Design, synthesis, and evaluation of curcumin derivatives as Nrf2 activators and cytoprotectors against oxidative death, *European Journal of Medicinal Chemistry* (2017), doi: 10.1016/j.ejmech.2017.04.008.

This is a PDF file of an unedited manuscript that has been accepted for publication. As a service to our customers we are providing this early version of the manuscript. The manuscript will undergo copyediting, typesetting, and review of the resulting proof before it is published in its final form. Please note that during the production process errors may be discovered which could affect the content, and all legal disclaimers that apply to the journal pertain.

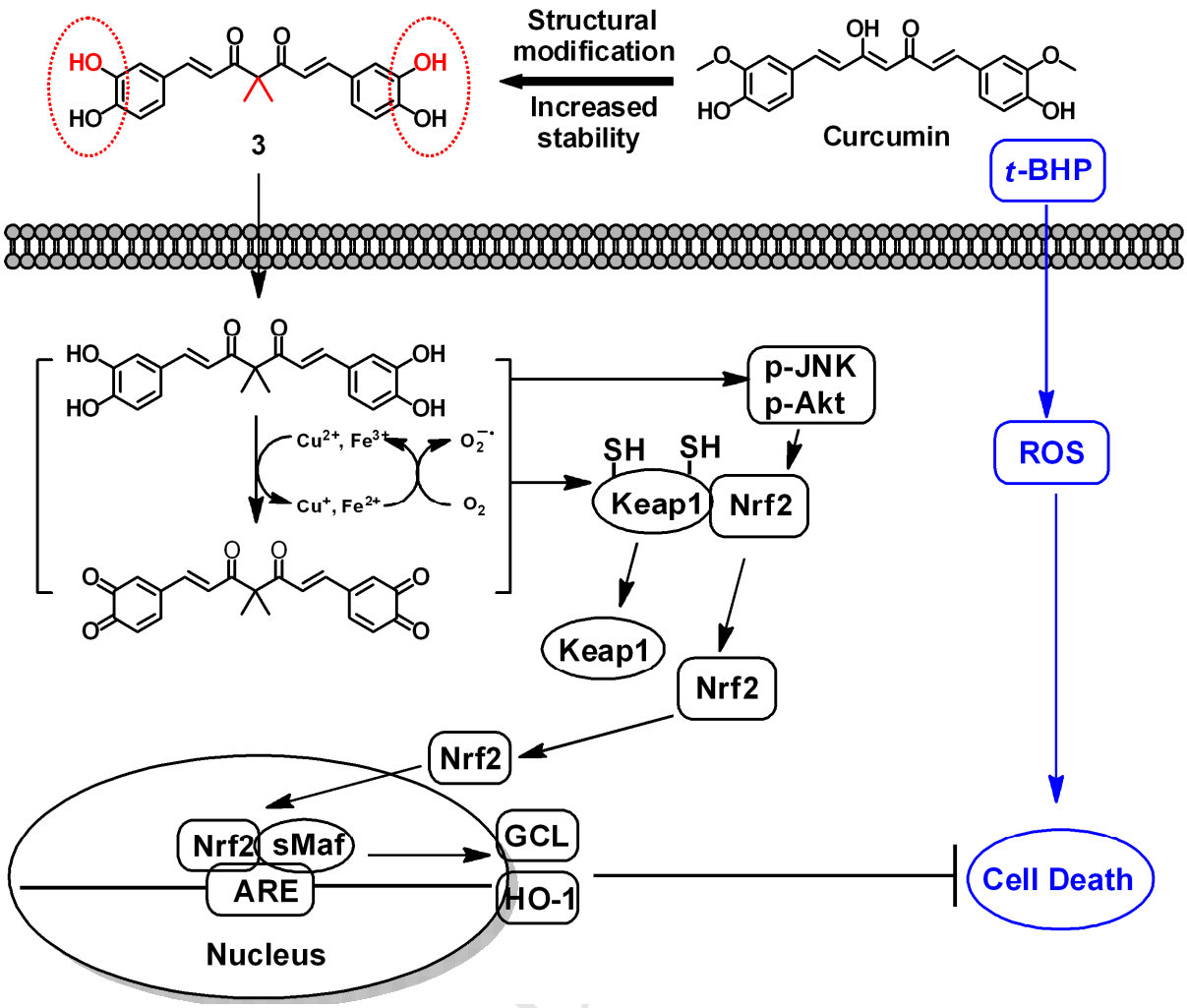
HO
HO
OH
OH
3
Structural modification
Increased stability
OH
O
HO
O
OH
Curcumin
t-BHP
HO
HO
OH
OH
Cu2+, Fe3+
O2−•
Cu+, Fe2+
O2
p-JNK
p-Akt
SH
SH
Keap1
Nrf2
ROS
Keap1
Nrf2
Nrf2
Nrf2
sMaf
ARE
GCL
HO-1
Nucleus
Cell Death

ACCEPTED

ACCEPTED MANUSCRIPT

Design, synthesis, and evaluation of curcumin derivatives as Nrf2 activators and cytoprotectors against oxidative death

Zhi-Shan Tu, Qi Wang, Dan-Dan Sun, Fang Dai*, Bo Zhou*

State Key Laboratory of Applied Organic Chemistry, Lanzhou University, 222 Tianshui Street S., Lanzhou, Gansu 730000, China

* Corresponding author.

E-mail: bozhou@lzu.edu.cn; daifang@lzu.edu.cn

Fax: +86-931-8915557

ACCEPTED MANUSCRIPT

Abstract

Activation of nuclear factor erythroid-2-related factor 2 (Nrf2) has been proven to be an effective means to prevent the development of cancer, and natural curcumin stands out as a potent Nrf2 activator and cancer chemopreventive agent. In this study, we synthesized a series of curcumin analogs by introducing the geminal dimethyl substituents on the active methylene group to find more potent Nrf2 activators and cytoprotectors against oxidative death. The geminally dimethylated and catechol-type curcumin analog (compound **3**) was identified as a promising lead molecule in terms of its increased stability and cytoprotective activity against the *tert*-butyl hydroperoxide (*t*-BHP)-induced death of HepG2 cells. Mechanism studies indicate that its cytoprotective effects are mediated by activating the Nrf2 signaling pathway in the Michael acceptor- and catechol-dependent manners. Additionally, we verified by using copper and iron ion chelators that the two metal ion-mediated oxidations of compound **3** to its corresponding electrophilic *o*-quinone, contribute significantly to its Nrf2-dependent cytoprotection. This work provides an example of successfully designing natural curcumin-directed Nrf2 activators by a stability-increasing and proelectrophilic strategy.

Keywords: Nrf2, curcumin, cytoprotective activity, Michael acceptor, catechol

ACCEPTED MANUSCRIPT

1. Introduction

Nuclear factor erythroid-2-related factor 2 (Nrf2) is an imperative regulator of cellular resistance against electrophilic and oxidative stress by activating phase II detoxifying and antioxidant enzymes such as hemeoxygenase-1(HO-1), glutathione S-transferase (GST), γ-glutamylcysteine synthetase (γGCS) and γ-glutamyl cysteine ligase (γ-GCL) [1]. In its inactive state, the basic leucine zipper protein (bZIP) transcription factor is associated with a Kelch-like ECH-associated protein 1 (Keap1) and sequestered in the cytoplasm, which facilitates its ubiquitination and proteasomal degradation. Once cells are exposed to oxidative or electrophilic stress, the active cysteine residues in Keap1 are covalently modified, resulting in Nrf2 disassociation from Keap1, thereby causing it stabilization and translocation to the nucleus. Accordingly, the Nrf2 accumulates in the nucleus, dimerizes with obligatory partner sMaf, and subsequently transactivates antioxidant response element (ARE)-driven phase II detoxifying and antioxidant genes [2-4]. In addition, numerous studies also indicate that diverse protein kinases including mitogen-activated protein kinase (MAPK), phosphatidylinositol 3-kinase (PI3K) and protein kinase C are involved in the Nrf2 transcriptional activation [5, 6].

Nrf2 has been identified as a potential molecular target for cancer chemoprevention and this has sparked the increasing interest in identifying and developing natural product-derived chemopreventive agents by targeting the keap1-Nrf2/ARE pathway [4, 7]. Curcumin (Fig. 1) is a renowned natural polyphenolic compound that isolated

from the rhizome of *Curcuma longa*. It has shown diverse biological activities including antioxidant, anti-inflammatory and anticancer activities [8, 9]. Although the precise mechanisms involved in its various activities remains to be elucidated, the antioxidant capacity of this molecule seems to be an element underlying its versatile biological properties. By virtue of its two phenolic groups and the β-diketone moiety, curcumin is known to directly scavenge the reactive oxygen species (ROS) [10, 11]. Moreover, due to the electrophilic characteristics of the Michael acceptor moieties, it can also act as an indirect antioxidant by activating the Keap1-Nrf2/ARE signaling pathway, which is crucial for cytoprotection against various forms of stress [12, 13]. Unfortunately, the clinical application of curcumin has been retarded by its poor bioavailability due to its low solubility in aqueous solutions and instability under physiological conditions [9, 14]. To deal with these drawbacks, numerous approaches have been undertaken including changing the keto-enol moiety into monocarbonyl or heterocyclic moiety, and substitution at central methylene carbon and so on [9, 15, 16]. Among these approaches, the geminal dimethylation on the central methylene carbon has been verified as an efficient modification strategy to improve pharmacological activities of curcumin [16-18]. Specifically, introduction of two hydrophobic methyl groups results in increased stability and anticancer activity [16], antioxidative activity [17] and water-solubility [18].

Thus, we synthesized a panel of curcumin analogs by insertion of dimethyl substituents on the active methylene group of curcumin (Fig. 1) to find more effective Nrf2

activators than the parent molecule. Moreover, we have previously identified a catechol-type resveratrol analog as a proelectrophile that is converted intracellularly into its corresponding electrophilic *o*-quinone by copper ions. The copper-ion mediated oxidation is indispensible for its cytoprotective activity against the oxidative death by activating Nrf2 [19]. Therefore, the catechol moiety was also considered to introduce into the geminal dimethyl substituted-curcumin analogs. The further modification generated compound **3** (Fig. 1), a catechol-type and geminally dimethylated curcumin analog. In view of this molecule containing two active sites (the Michael acceptor and catechol units), we further synthesized its reduced analog (**3-H**) and catechol-omitting analog (**10**) to clarify whether the two units are crucial for its Nrf2-dependent cytoprotective activity.

Figure 1 here

2. Results

2.1 Chemical Synthesis

Compounds **1-10** were synthesized according to the route shown in Scheme 1, with commercially available aromatic aldehydes as the starting materials. The aromatic aldehydes containing relatively active phenolic hydroxyl group were first protected by methoxymethyl chloride (MOMCl) or *tert*-butyldimethylsilyl chloride (TBSCl). The classical 1, 3-diketones (intermediates **2**) were synthesized by the aldol condensation of the modified benzaldehydes with acetylacetone according to the Pabon reaction

105 [20]. Then the final products **2, 4–8** and **10** were synthesized by the substitution of
106 iodomethane. Compounds **1, 3** and **9** bearing the relatively active phenolic hydroxyl
107 group were obtained by removing the MOM or TBS groups in the final step. Com-
108 pound **3-H** was synthesized by catalytic hydrogenation of compound **3** over Pd/C.

109 **Scheme 1 here**

110 *2.2 Stability assay of curcumin and its analogs*

111 Stability of the selected compounds (40 μM) in PBS (pH 7.4) was assessed by
112 monitoring their UV–visible absorption changes at 25 °C. As shown in Fig. 2, cur-
113 cumin was rapidly degraded in PBS within 30 min, while the geminally dimethylat-
114 ed curcumin, compound **1**, showed no signs of decomposition over a 30 min period.
115 These results demonstrate that geminal dimethylation on the central methylene group
116 improves the stability of curcumin. Notably, compound **3** was also stable under the
117 same conditions, whereas methylation and dehydroxylation of the two catechol moi-
118 eties in compound **3** to generate compounds **2** and **10**, respectively, led to significant
119 decomposition. These data suggest that the catechol moieties of compound **3** are also
120 essential for its stability.

121 **Figure 2 here**

122 *2.3 SAR analysis for the cytoprotection of curcumin and its analogs*

123 The *t*-BHP-induced oxidative death of HepG2 cells was employed as a model to
124 evaluate the cytoprotective activity of curcumin and its analogs [21, 22]. Specifically,
125 the cells were pretreated with the test compounds at nontoxic concentration (5 μM)

126 (Fig. 3A) for 24 h followed by their removal and a subsequent challenge with 900 μM
127 *t*-BHP. As shown in Fig 3B, exposure of the cells to *t*-BHP for 6 h resulted in about
128 70% cell death, but pretreatment with 5 μM curcumin and its analogs attenuated cell
129 death induced by *t*-BHP. Most of the analogs were more potent cytoprotective agents
130 than the parent curcumin. A comparison of cytoprotection between curcumin and
131 compound **1** clearly indicates that geminal dimethylation on the central methylene
132 carbon of curcumin enhanced significantly its activity. Furthermore, demethylation of
133 compound **1** to produce the catechol-type compound **3** resulted in an enhanced cyto-
134 protection. On the contrary, abrogating the catechol (compound **10**) or Michael ac-
135 ceptor (**3-H**) moieties of compound **3** led to an obvious reduction in the cytoprotec-
136 tion. These results indicate that both the catechol and Michael acceptor moieties are
137 essential for recapitulating the cytoprotective activity observed for compound **3**.

138 **Figure 3 here**

139 *2.4. Compound **3** attenuated dose-dependently the cell death and ROS accumulation*
140 *induced by t-BHP*

141 Considering that compound **3** was the most prominent one among the test mole-
142 cules, its cytoprotective activity at different concentrations was subsequently meas-
143 ured by the MTT assay. As shown in Fig. 4A, treatment with *t*-BHP induced about
144 70% cell death, but pretreatment of the cells with compound **3** (1.25, 2.5 and 5 μM)
145 protected does-dependently the cells from oxidative death. Since *t*-BHP can be me-
146 tabolized to free radical intermediates by cytochrome P-450, ultimately resulting in

147 oxidative stress [22], the extent of ROS generation induced by *t*-BHP was monitored
148 by flow cytometry using DCFH-DA. Treatment with 900 μM *t*-BHP for 3 h resulted
149 in 2.5-fold increase in the ROS levels relative to the control. In contrast, compound **3**
150 suppressed dose-dependently the ROS accumulation (Fig. 4B). Remarkably, the test
151 procedure, pretreatment with compound **3** followed by its removal, hints at the possi-
152 bility that this molecule can penetrate into the cells and function as an indirect anti-
153 oxidant to activate endogenous antioxidative defense system.

154 **Figure 4 here**

155 *2.5. Compound **3** activated Nrf2 and its downstream genes in HepG2 cells*

156 Under activation in response to oxidative and electrophilic stress, Nrf2 detaches
157 from Keap1, translocates to the nucleus and ultimately activates transcription of phase
158 II detoxifying enzymes [1]. Therefore, we next examined the expression of Nrf2 and
159 its downstream phase II detoxifying enzymes induced by compound **3**. It can be seen
160 from Fig. 5A that after exposing the cells to 5 μM compound **3**, both nuclear and cy-
161 tosolic levels of Nrf2 were increased as early as 1 h, to a peak value at 3–6 h, and then
162 gradually decreased to a basal level after 12 h. Additionally, 3 h treatment with com-
163 pound **3** under different concentrations (1.25, 2.5 and 5 μM) increased
164 dose-dependently the Nrf2 expression (Fig. 5B). Likewise, a time- and
165 dose-dependent effects could be also observed for the expression of phase II detoxi-
166 fying enzymes (including HO-1, GCLC and GCLM) induced by compound **3** (Fig. 5C
167 and D). Furthermore, *tert*-butyl hydroquinone (*t*-BHQ), a well-known Nrf2 activator,

168 was employed as a positive control. When compared with *t*-BHQ, compound **3** was a
169 more effective cytoprotector and Nrf2 activator since only 5 μM compound **3** showed
170 a similar effect observed for 20μM *t*-BHQ in the cytoprotection (Fig. 5E) and Nrf2
171 activation (Fig. 5F) and its downstream gene expression (Fig. 5G).

172 **Figure 5 here**

173 To further confirm the cytoprotection of compound **3** toward HepG2 cells depend
174 on the Nrf2 activation and its downstream gene expression, the cytoprotection assay
175 was checked again in the presence of trigonelline (TRG) (an Nrf2 inhibitor) [23, 24],
176 Zinc protoporphyrin IX (ZnPP) (a HO-1 inhibitor) or L-buthionine-(S,R)-sulfoximine
177 (BSO) (a GCL inhibitor). Pretreatment with TRG, ZnPP and BSO attenuated obvi-
178 ously the cytoprotective activity of compound **3** (Fig. 6). These above results support
179 the conclusion that compound **3** ameliorates the *t*-BHP-induced death of HepG2 cells
180 through activating Nrf2, highlighting its role as an efficient Nrf2 activator and thereby
181 as an indirect antioxidant.

182 **Figure 6 here**

183 *2.6 Compound **3** induced phosphorylation of Akt and JNK*

184 It is known that MAPKs including JNKs and ERKs, as well as PI3K/Akt pathways
185 play a role in the Nrf2 transcriptional activation [5, 6]. The influence of compound **3**
186 on the MAPKs and PI3K/Akt pathways was thus studied. It can be seen from Western
187 bolt results that treatment with compound **3** showed no benefit on phosphorylation of
188 ERK, but increased time-dependently that of p-Akt within 120 min. In addition,

compound **3** stimulated a time-dependent increase of JNK phosphorylation and a maximal response occurred at 30 min (Fig. 7A). In contrast, pretreatment with SP600125 (a JNK inhibitor) or LY294002 (a specific PI3K/Akt inhibitor) inhibited markedly the cytoprotection (Fig. 7B) and the expression of phase II detoxifying enzymes including HO-1, GCLC and GCLM (Fig. 7C) induced by compound **3**. Base on the above results, we can conclude that the cytoprotection of compound **3** is mediated, at least in part, by a JNK and PI3K/Akt-dependent activation of Nrf2.

Figure 7 here

*2.7 Compound **3** activated Nrf2 in a Keap1-dependent manner*

Normally, Nrf2 is sequestered by the Keap1 protein in the cytoplasm. Once cells are exposed to oxidative or electrophilic stress, the active cysteine residues in Keap1 are covalently modified, thereby facilitating the release of Nrf2 and its transcriptional activation [25, 26]. Previous reports have shown that the Michael acceptors could directly conjugate with the active cysteine residues of Keap1, resulting in dissociation and nuclear translocation of Nrf2 [4, 27]. Usually, the reaction can be quenched by DTT, a sulfhydryl-containing Michael acceptor abrogating agent [28, 29]. To ascertain whether compound **3** induces Nrf2 activation in Michael acceptor- and Keap1-dependent manners, we tested initially the expression of Nrf2 by Western blotting coupled with the use of DTT. The increased Nrf2 expression induced by compound **3** can be reversed by pretreatment with DTT (Fig. 8A), implying that compound **3** induces Nrf2 activation at least partially in a Michael acceptor-dependent

210 manner. Furthermore, the decreased Keap1 band in response to the treatment of com-
211 pound **3** can be reversed obviously by DTT (Fig. 8B). This is in tune with the results
212 from Li and coworkers, showing that an increase in the expression of Nrf2 based on
213 exposure of 2-*tert*-butyl-1,4-hydroquinone was accompanied with a decreased levels
214 of Keap1 [30], and highlights that the Nrf2 activation is also Keap1-dependent.

215 **Figure 8 here**

216 *2.8 Compound **3** enhanced Nrf2 stability*

217 Under basal conditions, Nrf2 is constantly targeted for Keap1-dependent ubiquiti-
218 nation and subsequent proteasomal degradation to maintain its low levels in the cells
219 [26]. Molecules bearing Michael acceptor unit can react with the active cysteine resi-
220 dues of Keap1 and thus suppress Nrf2 ubiquitination and subsequent proteasomal
221 degradation [4, 27, 31]. To investigate whether compound **3** could stabilize Nrf2 lev-
222 els, the expression of total Nrf2 was tested by Western blotting. Compound **3** stimu-
223 lated a time-dependent expression of Nrf2 in HepG2 cells with a maximal response
224 within 3 h (Fig. 8C). Moreover, we quantified directly the turnover rate of Nrf2 by
225 using cycloheximide (a protein synthesis inhibitor) as a means to block protein syn-
226 thesis [32]. As shown in Fig. 8D, after exposing the cells to CHX, the total Nrf2 levels
227 were significantly decreased in an hour, whereas pretreatment with compound **3**
228 slowed obviously the turnover rate. A single-phase decay model [32] to fit the data
229 revealed that pretreatment of compound **3** prolonged the half-life of Nrf2 protein from
230 22 to 57 min, approximately 2.6 times longer than the control group (Fig. 8E). These

results demonstrate that compound **3** can significantly improve the Nrf2 stability through suppressing its degradation.

2.9 Both the catechol and Michael acceptor moieties are important for the cytoprotection and Nrf2 activation

In the presence of oxygen and transition metal ions, catechol proelectrophiles can be easily oxidized to its corresponding *o*-quinone electrophiles, which subsequently undergo Michael addition with Keap1 and activate the Keap1-Nrf2/ARE pathway [4, 33]. Redox-active metal such as copper and iron are essential to all organisms living and crucial for the function of several metalloenzymes involved in oxidation metabolism [19, 33-35]. Our previous study has shown that a catechol-type resveratrol analog could be converted intracellularly into its corresponding *o*-quinone by copper ions. The oxidative conversion is required for its Nrf2 activation [19]. Therefore, effect of various metal ion chelating agents on the cytoprotection of compound **3** was investigated to clarify the mechanism by which compound **3** is oxidized, and to confirm whether its corresponding *o*-quinone is responsible for the cytoprotection. As shown in Fig. 9A, pretreatment with the wide variety of metal ion chelator ethylenediaminetetraacetic acid (EDTA) attenuated significantly the cytoprotection, suggesting a role of metal ions involved in oxidation of compound **3**. Furthermore, both the iron chelator desferrioxamine (DFO) (Fig. 9A) and the copper chelator neocuproine (NEO) (Fig. 9B) inhibited obviously its cytoprotection. These results demonstrate that both the copper and iron ions could mediate oxidations of the catechol-type compound **3** to

its corresponding electrophilic *o*-quinone, thereby contributing significantly to the Nrf2-dependent cytoprotection. This is further supported by relatively weaker Nrf2 activation and expression of its downstream genes by the catechol-omitting analog (compound **10**) than by compound **3** (Fig. 9C).

Additionally, a comparison of cytoprotection (Fig. 3B) along with protein expression of Nrf2 (Fig. 9C) and its downstream genes (Fig. 9D) between compound **3** and its reduced analog (**3-H**), clearly indicates that the Michael acceptor units are necessary for the cytoprotection. To further clarify the role of the Michael acceptor moieties, the effect of DTT on the compound **3**-induced cytoprotection and Nrf2 activation was evaluated. Pretreatment with DTT abrogated remarkably the cytoprotection (Fig. 9B) and Nrf2 activation (Fig. 8A). Based on these data, we can infer that both the catechol and Michael acceptor moieties are important for the Nrf2-dependent cytoprotection.

Figure 9 here

3. Discussion

Nrf2, a potential molecular target for cancer prevention, has attracted much attention in discovering and developing natural product-derived chemopreventive agents by targeting the Keap1-Nrf2/ARE pathway [4, 7]. Most of Nrf2 activators belong to the chemical class of electrophiles [7]. However, the intrinsic reactivity of electrophiles is also associated with augmented metabolic degradation and toxicity, due to reactions with nontarget proteins and other compounds such as glutathione [4,

36]. Therefore, a proelectrophilic strategy to design Nrf2 activators by introduction of the catechol or hydroquinone moiety is suggested because the proelectrophiles manifest fewer side effects [37, 38]. Our previous study shows a catechol-type resveratrol analog intracellularly converted into its *o*-quinone electrophile by copper ions, and the copper-mediated oxidation is necessary to its Nrf2 activation and subsequent cytoprotection [19]. Accordingly, we designed a series of natural curcumin (a potent Nrf2 activator [13, 39]) analogs by introduction of the geminal dimethyl groups and the catechol moieties to find more effective Nrf2 activators based on a stability-increasing and proelectrophilic strategy.

In tune with the previous result [16], introduction of the geminal dimethyl substituents does improve the stability of curcumin (Fig. 2). Furthermore, a striking feature of our data is that the catechol moieties can further stabilize the curcumin analogs as exemplified in compound **3**. We reasoned that the phenolic hydroxyl of compound **3** can readily undergo deprotonation to yield phenoxide anion under physiological pH conditions, resulting in delocalization of negative charge over its cinnamoyl part and subsequent prevention from attacking by H_2O.

Subsequently, this molecule turned out to be superior to other compounds in terms of its increased stability and cytoprotective activity against the oxidative death. Mechanism studies indicate that the excellent cytoprotection of compound **3** is attributed to its facilitating nuclear translocation of Nrf2 (Fig. 5A and B) and subsequent expression of Nrf2-driven antioxidants including HO-1, GCLM, GCLC (Fig.

294 5C and D). These results were further supported by using the Nrf2 inhibitor (TRG)
295 and HO-1, GCL inhibitor (ZnPP and BSO, respectively) (Fig. 6). Western blot results
296 indicate that compound **3** induces Nrf2 activation in a Keap1-dependent manner (Fig.
297 8B) and increases remarkably its stability (Fig. 8D). This allows Nrf2 to escape form
298 degradation and translocate to nuclear, resulting the Nrf2 target gene expression.
299 Moreover, the cytoprotection of compound **3** is mediated, at least in part, by JNK and
300 PI3K/Akt-dependent activation of Nrf2 (Fig. 7A), which is supported by the reduced
301 cytopretection in the presence of a JNK inhibitor (SP600125) or an Akt inhibitor
302 (LY294002) (Fig. 7B and C).

303 The essential question considered here is to clarify the role of the Michael acceptor
304 and catechol units for compound **3** that make it viable Nrf2 activator. The MTT data
305 (Fig. 3B) coupled with the Western blot results (Fig. 9C and D) suggest that the Mi-
306 chael acceptor units are crucial for maintaining its Nrf2-dependent cytoprotection be-
307 cause reduction of olefin (**3-H**) or pretreatment of DTT (Fig. 9B) lead to a significant
308 decrease in the potency. Furthermore, the oxidation of the catechol-type compound **3**
309 by intracellular copper and iron ions is also required for its Nrf2-dependent cytopro-
310 tection. This could be explained by the attenuated cytoprotction by using NEO and
311 DFO **(**Fig. 9A and B**)** and the reduced potency in the case of compound **10** (Fig. 3B,
312 9C and D). it should be pointed out that this result distinguishes our previous result in
313 the case of a catechol-type resveratrol analog where the intracellular copper rather
314 than iron ions are responsible for its oxidation [19]. In fact, Cu(II)/Cu(I) (E^o = +0.15

V) redox couple is relatively easier to favor redox cycle than the Fe(III)/Fe(II) (E^o = +0.77 V) redox couple [40]. Therefore, involvement of iron ions should be compound-dependent, probably due to the lower redox potential of compound **3** compared with that of the catechol-type resveratrol analog. This is in concert with the previous studies that iron ions catalyze the wine polyphenols containing catechol or pyrogallol moieties to form *o*-quinones [41, 42]. Generally, the hydroxylated curcuminoids work as antioxidants but as prooxidants under special conditions such as high concentrations and in the presence of cupric ions [43]. In fact, this study highlights the fact that catechol-type compound **3** makes use of endogenous copper and iron ions to construct an efficient prooxidant system, resulting in formation of electrophilic *o*-quinone and Nrf2-dependent cytoprotection. In other words, in the current case, compound **3** plays finally a role of indirect antioxidant by its prooxidant activity.

4. Conclusion

This work provides useful information for using a stability-increasing and proelectrophilic strategy to develop a curcumin-inspired Nrf2 inducer. Based on this strategy, the catechol-type compound **3** has been identified as a promising lead molecule in terms of its increased stability and excellent cytoprotective activity. It could effectively disrupt the Nrf2-Keap1 complex and thereby increase the expression of phase II detoxifying enzymes in the Michael acceptor- and catechol-dependent manners (Fig. 10). Using copper and iron ion chelating agents, we verified that this molecule could

make use of the two intracellular ions to produce its corresponding *o*-quinone, thereby contributing to its Nrf2-dependent cytoprotection. In addition, the activation of the JNK and PI3K pathways as well as stabilization of Nrf2 by this molecule was also responsible for its Nrf2-dependent cytoprotection.

Figure 10 here

5. Experimental section

5.1 General information

Roswell Park Memorial Institute (RPMI)-1640, zinc protoporphyrin IX (ZnPP), L-buthionine-(S,R)-sulfoximine (BSO), SP600125 and cycloheximide (CHX) were obtained from Sigma (St. Louis, MO, USA). LY294002, Cell lysis buffer for Western and IP, BCA protein assay kit, 2′,7′-Dichlorofluorescin diacetate (DCFHDA), 3-(4, 5-dimethylthiazol-2-yl)-2,5-diphenyltetrazolium bromide (MTT) and phenylmethanesulfonyl fluoride were from Beyotime Institute of Biotechnology (Jiangsu, China). Keap1, β-actin, Nrf2 and Lamin A were purchased from Santa Cruz Biotechnology (CA, USA). Rabbit polyclonal antibody to HO-1 was purchased from Enzo Life Sciences (NY, USA). Rabbit antibodies against glutamate cysteine ligase catalytic subunit (GCLC) and glutamate cysteine ligase modulatory subunit (GCLM) were purchased from Abcam (Shanghai, China). All the phosphorylated, nonphosphorylated kinase antibodies used in this study and glyceraldehyde 3-phosphate dehydrogenase (GAPDH) were obtained from Cell Signaling Technology (Danvers, MA,

USA). HRP-labeled secondary antibody was obtained from TransGen Biotech Co., Ltd. (Beijing, China). All other chemicals were of the highest quality available.

5.2 Synthesis

Synthesis of curcumin and its designed analogs was conducted according to the route described in Scheme 1 and the details are described as below. Their structures were confirmed by ^{1}H and ^{13}C NMR spectra and ESI-MS analysis (See also the supplementary data).

5.2.1. TBS protection of hydroxyl groups [44]

Tert-butyldimethylsilyl chloride (TBSCl) (1.2 eq) and imidazol (3 eq) were added to a solution of isovanillin or 3,4-dihydroxybenzaldehyde in CH_2Cl_2 (0.25 M) at 0 °C. The mixture was warmed to room temperature and stirred for 6 h. The solution was washed with saturated Na_2CO_3, brine and dried over Na_2SO_4, and concentrated under reduced pressure to afford the crude product as a white solid which was used to next step directly.

5.2.2. MOM protection of hydroxyl groups [45]

To a solution of 2-hydroxybenzaldehyde (1.0 eq) in anhydrous THF (0.25 M) was added a suspension of 60% w/w NaH (1.2 eq) in THF, the mixture was stirred at room temperature for 1 h. Then chloromethyl methyl ether (MOMCl) (1.2 eq) was added, and the mixture was stirred at room temperature for 2 h followed by quenching and extraction with ethyl acetate. The organic layer was washed with brine, 5% NaOH, dried over Na_2SO_4, and concentrated under reduced pressure to afford the crude prod-

uct as a white solid which was used to next step directly.

*5.2.3.General procedure for synthesis of intermediates **1**, **3** and **4** [20]*

To a solution of acetyl acetone (2 eq) in ethyl acetate was added boric anhydride (1.2 eq) and tributyl borate (4.8 eq). The mixture was heated to 50 °C and stirred for 30 min. Then a solution of appropriate benzaldehyde (4 eq) in ethyl acetate was added, followed by slow addition of n-butylamine (4 eq). After refluxing for 6 h, the solution was cooled to room temperature and diluted with 1 N HCl. The yellow-orange solid was suspended in water, filtered, and dried under vacuum. All crude compounds were recrystallized in ethyl acetate to give the pure products.

*5.2.4. General procedure for synthesis of compounds **2**, **4-8** and **10** [20]*

To a stirring solution of intermediate **3** (1.0 eq) in CH_2Cl_2 (0.25 M) was added a mixture of NaOH (2.4 eq) and tetrabutylammonium chloride in water under ice bath. The mixture was warmed to room temperature and stirred for 30 min followed by addition of methyl iodide (3.6 eq). After refluxing for 2 h, the solution was cooled to room temperature and poured into water, adjusted pH to 4~5 with 1 N HCl and extracted with CH_2Cl_2. The organic layer was washed with brine, dried over Na_2SO_4, and concentrated under reduced pressure. The residue was purified by silica gel column chromatography petroleum ether/acetone (3/1, v/v) to afford the target molecule.

*(1E, 6E)-1, 7-bis(3, 4-dimethoxyphenyl)-4, 4-dimethylhepta-1,6-diene-3, 5-dione (**2**).*

Compound **2** was prepared according to the general procedure, using (1E, 4Z, 6E)-1, 7-bis(3, 4-dimethoxyphenyl)-5-hydroxyhepta-1, 4, 6-trien-3-one (396.4 mg, 1.0 mmol)

to obtain pure compound **2** as a yellow solid (186.8 mg, yield 44%); mp 69-71 °C; ^{1}H NMR (400 MHz, Acetone-d_6): δ = 7.63 (d, J = 15.6 Hz, 2H), 7.34 (d, J = 2.0 Hz, 2H), 7.25 (dd, J = 8.0 Hz, 2.0 Hz, 2H), 6.98 (d, J = 8.0 Hz, 2H), 6.92 (d, J = 15.6 Hz, 2H), 3.85 (s, 6H),3.83 (s, 6H), 1.42 (s, 6H); ^{13}C NMR (100 MHz, Acetone-d_6)： δ = 197.5, 152.0, 149.6, 143.4, 127.4, 123.4, 119.6, 111.4, 110.6, 56.0, 55.2, 55.2, 20.6; MS (ESI): (m/z) = 424.9 $[M + H]^+$.

*(1E, 6E)-4, 4-dimethyl-1, 7-bis(3, 4, 5-trimethoxyphenyl)hepta-1, 6-diene-3, 5-dione (**4**)*. Compound **4** was prepared according to the general procedure, using (1E, 4Z, 6E)-5-hydroxy-1, 7-bis(3, 4, 5-trimethoxyphenyl)hepta-1, 4, 6-trien-3-one (456.5 mg, 1.0 mmol) to obtain pure compound **4** as a yellow solid (266.5 mg, yield 51%); mp 83-85 °C; ^{1}H NMR (400 MHz, Acetone-d_6): δ = 7.62 (d, J = 15.6 Hz, 2H),7.06 (s, 4H), 7.00 (d, J = 15.6 Hz, 2H), 3.85 (s, 12H), 3.75 (s, 6H), 1.43 (s, 6H); ^{13}C NMR (100 MHz, Acetone-d_6)： δ = 197.5, 153.7, 143.5, 140.7, 130.0, 121.1, 106.2, 60.0, 59.7, 55.6, 20.5; MS (ESI): (m/z) = 484.4 $[M + H]^+$.

*(1E, 6E)-1, 7-bis(3-methoxyphenyl)-4, 4-dimethylhepta-1, 6-diene-3, 5-dione (**5**)*. Compound **5** was prepared according to the general procedure, using (1E, 4Z, 6E)-5-hydroxy-1, 7-bis(3-methoxyphenyl)hepta-1, 4, 6-trien-3-one (336.1 mg, 1.0 mmol) to obtain pure compound **5** as a yellow solid (160.3 mg, yield 44%); mp 63-65 °C; ^{1}H NMR (400 MHz, Acetone-d_6): δ = 7.66 (d, J = 15.6 Hz, 2H), 7.33 (t, J = 7.6 Hz, 2H), 7.29-7.27 (m, 4H), 7.08 (d, J = 15.6 Hz, 2H),7.00 (ddd, J = 7.6, 2.4, 1.2 Hz, 2H), 3.82 (s, 6H), 1.47 (s, 6H); ^{13}C NMR (100 MHz, Acetone-d_6)： δ = 197.7,

160.2, 143.1, 136.0, 129.9, 122.2, 121.1, 116.6, 113.3, 60.1, 54.8, 20.4; MS (ESI): (m/z) = 365.0 $[M + H]^+$.

*(1E,6E)-1,7-bis(2,6-dimethoxyphenyl)-4,4-dimethylhepta-1,6-diene-3,5-dione (**6**)*. Compound **6** was prepared according to the general procedure, using 2,6-methoxybenzaldehyde (396.4 mg, 1.0 mmol) to obtain pure compound **6** as a yellow oil (199.5 mg, yield 47%); mp 165-167 °C; ^{1}H NMR (400 MHz, $CDCl_3$): δ = 8.15 (d, J = 16 Hz, 2H), 7.28-7.20 (m, 6H), 6.49 (d, J = 8.4 Hz, 4H), 3.81 (s, 12H),1.44 (s, 6H); ^{13}C NMR (100 MHz, $CDCl_3$): δ= 200.2, 160.4, 134.0, 131.3, 125.3, 112.7, 103.6, 60.7, 55.8, 21.3; MS (ESI): (m/z) = 425.0 $[M + H]^+$.

*(1E, 6E)-1, 7-bis(2-methoxyphenyl)-4, 4-dimethylhepta-1, 6-diene-3, 5-dione (**7**)*. Compound **7** was prepared according to the general procedure, using (1E, 4Z, 6E)-5-hydroxy-1, 7-bis(2-methoxyphenyl)hepta-1, 4, 6-trien-3-one (336.4 mg, 1.0 mmol) to obtain pure compound **7** as a yellow solid (156.7 mg, yield 43%); mp 124-125 °C; ^{1}H NMR (400 MHz, Acetone-d_6): δ = 8.03 (d, J = 15.6 Hz, 2H), 7,69 (dd, J = 7.6 Hz, 1.6 Hz, 2H), 7.41 (ddd, J = 8.4, 7.6, 1.6 Hz, 2H), 7.07 (d, J = 8.4 Hz, 2H), 7.05 (d, J = 15.6 Hz, 2H), 6.97 (t, J = 7.6 Hz, 2H), 3.91 (s, 6H), 1.45 (s, 6H); ^{13}C NMR (100 MHz, Acetone-d_6): δ = 197.8, 158.8, 138.0, 132.1, 128.6, 123.0, 122.2, 120.7, 111.5, 60.2, 55.1, 20.5; MS (ESI): (m/z) = 365.1 $[M + H]^+$.

*(1E, 6E)-4, 4-dimethyl-1, 7-bis(2-(trifluoromethyl)phenyl)hepta-1, 6-diene-3, 5-dione (**8**)*. Compound **8** was prepared according to the general procedure, using (1E, 4Z, 6E)-5-hydroxy-1, 7-bis(2-(trifluoromethyl)phenyl)hepta-1, 4, 6-trien-3-one (412.3 mg,

1.0 mmol) to obtain pure compound **8** as a yellow solid (140.9 mg, yield 32%); mp 61-63 °C; ^{1}H NMR (400 MHz, Acetone-d_6): δ = 8.06 (d, J = 7.6 Hz, 2H), 8.02 (d, J = 15.6 Hz, 2H), 7.82 (d, J = 7.6 Hz, 2H), 7.72 (t, J = 7.6 Hz, 2H),7.65 (t, J = 7.6 Hz, 2H), 7.19 (d, J = 15.6 Hz, 2H), 1.54 (s, 6H); ^{13}C NMR (100 MHz, Acetone-d_6)：δ = 197.54, 137.75, 137.73; MS (ESI): (m/z) = 440.9 $[M + H]^+$.

*(1E, 6E)-4, 4-dimethyl-1, 7-diphenylhepta-1, 6-diene-3, 5-dione (**10**).* Compound **10** was prepared according to the general procedure, using (1E, 4Z, 6E)-5-hydroxy-1,7-diphenylhepta-1, 4, 6-trien-3-one (552.6 mg, 2.0 mmol) to obtain pure compound **10** as a yellow solid (182.6 mg yield 30%); mp 51-53 °C; ^{1}H NMR (400 MHz, Acetone-d_6): δ = 7.72-7.68 (m, 6 H), 7.44-7.40 (m, 6H), 7.08 (d, J = 15.6 Hz, 2H), 1.49 (s, 6H); ^{13}C NMR (100 MHz, Acetone-d_6)：δ = 197.7, 143.1, 134.6, 130.6, 128.9, 128.6, 121.9, 60.2, 20.4; MS (ESI): (m/z) = 305.9 $[M + H]^+$.

*5.2.5. General procedure for synthesis of compounds **1** and **3** [43]*

To a stirring solution of TBS-protected compound **1** or **3** in THF was added drop-wise a solution of tetrabutylammonium fluoride (1M) in THF at 0 °C. Once finished, the mixture was warmed to room temperature for 1 h. The mixture was poured into ice water, adjusted pH to 3~4 with 1 N HCl, then extracted with ethyl acetate. The organic layer was washed with brine, dried over Na_2SO_4, and concentrated under re-duced pressure. The residue was purified by silica gel column chromatography with petroleum ether/acetone (3/1, v/v) to afford the product.

(1E, 6E)-1,7-bis(4-hydroxy-3-methoxyphenyl)-4,4-dimethylhepta-1, 6-diene-3,

*5-dione (**1**)*. Compound **1** was prepared according to the general procedure, using (1E, 4Z, 6E)-1, 7-bis(4-((tert-butyldimethylsilyl)oxy)-3-methoxyphenyl)-5-hydroxyhepta-1, 4, 6-trien-3-one (1.194 g, 2.0 mmol) to obtain pure compound **1** as a yellow solid (261.6 mg, yield 33%); mp 142-144 °C; ^{1}H NMR (400 MHz, Acetone-d_6): δ = 8.28 (s, 1H), 7,62 (d, J = 15.6 Hz, 2H), 7.35 (d, J = 2.0 Hz, 2H), 7.19 (dd, J = 8.0 Hz, 2.0 Hz, 2H), 6.87 (d, J = 15.6 Hz, 2H), 6.86 (d, J = 8.0 Hz, 2H), 3.87 (s, 6H), 1.42 (s, 6H); ^{13}C NMR (100 MHz, Acetone-d_6)：δ = 197.4, 149.5, 147.8, 143.6, 126.6, 123.7, 119.1, 115.2, 111.0, 60.0, 55.4, 20.6; MS (ESI): (m/z) = 397.0 $[M + H]^+$.

*(1E, 6E)-1,7-bis(3, 4-dihydroxyphenyl)-4, 4-dimethylhepta-1, 6-diene-3, 5-dione (**3**)*. Compound **3** was prepared according to the general procedure, using (1E, 4Z, 6E)-1, 7-bis(3, 4-bis((tert-butyldimethylsilyl)oxy)phenyl)-5-hydroxyhepta-1, 4, 6-trien-3-one (797.4 mg, 1.0 mmol) to obtain pure compound **3** as a yellow solid (84.7 mg, yield 23%); mp 191-193 °C; ^{1}H NMR (400 MHz, Acetone-d_6): δ = 8.36 (s, 4H), 7.56 (d, J = 15.6 Hz, 2H), 7.16 (d, J = 2.0 Hz, 2H), 7.07 (dd, J = 8.0 Hz, 2.0 Hz, 2H), 6.85 (d, J = 8.0 Hz, 2H), 6.76 (d, J = 15.6 Hz, 2H), 1.42 (s, 6H); ^{13}C NMR (100 MHz, Acetone-d_6)：δ = 197.4, 148.3, 145.4, 143.5, 126.7, 122.5, 118.9, 115.5, 114.5, 60.0, 20.6; MS (ESI): (m/z) = 369.0 $[M + H]^+$.

*5.2.6. General procedure for synthesis of compound **9** [45]*

To a solution of MOM-protected compound **9** in MeOH (0.25 M) was added conc. HCl (0.1 M) over 10 min in ice bath. Then the mixture was warmed to room temperature, stirred for 2 h and concentrated under reduced pressure. The crude product was

483 further purified by silica gel column chromatography with petroleum ether /acetone
484 (3/1, v/v) to give compound **9** as a yellow solid.

485 *(1E, 6E)-1, 7-bis(2-hydroxyphenyl)-4, 4-dimethylhepta-1, 6-diene-3, 5-dione (**9**).*
486 Compound **9** was prepared according to the general procedure, using (1E, 4Z,
487 6E)-5-hydroxy-1, 7-bis(2-(methoxymethoxy)phenyl)hepta-1, 4, 6-trien-3-one (396.4
488 mg, 1.0 mmol) to obtain pure compound **9** as a yellow solid (117.7 mg, yield 35%);
489 mp 161-163 °C; ^{1}H NMR (400 MHz, Acetone-d_6): δ = 9.21 (s, 2H), 8.04 (d, J = 15.6
490 Hz, 2H), 7.62 (dd, J = 8.0 Hz, 1.6 Hz, 2H), 7.25 (td, J = 8.0, 16 Hz, 2H), 7.11 (d, J =
491 15.6 Hz, 2H), 6.95 (d, J = 8.0 Hz, 2H), 6.87 (t, J = 7.6 Hz, 2H), 1.45 (s, 6H); ^{13}C
492 NMR (100 MHz, Acetone-d_6)： δ = 197.9, 157.1, 138.6, 131.8, 129.2, 121.8, 121.5,
493 120.0, 116.2, 60.2, 20.6; MS (ESI): (m/z) = 337.2 $[M + H]^+$.

494 *5.2.7. General procedure for synthesis of compound **3-H** [46]***.**

495 A solution of compound **3** in methanol was added to a mixture of catalytic amount
496 Pd/C (10%) in methanol under hydrogen atmosphere. Then the reaction mixture was
497 stirred at room temperature for 8 h. The mixture was filtrated and the filtrate was
498 evaporated. The residue was further purified by silica gel column chromatography
499 with ethyl acetate/petroleum ether (5/1, v/v) to afford compound **3-H** as a yellow oil.

500 *1,7-bis(3,4-dihydroxyphenyl)-4,4-dimethylheptane-3,5-dione (**3-H**).*

501 Compound **3-H** was prepared according to the general procedure, using
502 (1E,6E)-1,7-bis(3,4-dihydroxyphenyl)-4,4-dimethylhepta-1,6-diene-3,5-dione (368.4
503 g, 1.0 mmol) to obtain pure compound **3-H** as a yellow oil. (52.6 mg, yield 14%); ^{1}H

NMR (400 MHz, Acetone-d_6): δ = 7.91 (s, 4H), 6.70 (d, J = 8.0 Hz, 2H), 6.64 (d, J = 2.0 Hz, 2H), 6.48 (dd, J = 8.0 Hz, 2.0 Hz, 2H), 2.63 (s, 8H), 1.24 (s, 6H); ^{13}C NMR (150 MHz, Acetone-d_6): δ = 208.7, 144.9, 143.2, 132.9, 119.5, 115.4, 115.1, 61.7, 40.2, 20.5; MS (ESI): (m/z) = 371.2 $[M - H]^-$.

5.3 Stability assay

The stability of curcumin and its analogs (40 μM) were assessed by monitoring their UV-visible absorption changes (interval = 2 min) in phosphate buffer solution (PBS) (pH 7.4) at 25 °C by a TU-1901 UV/Vis spectrophotometer (Beijing Purkinje General Instrument Co., Ltd., Beijing, China), Spectra were run against blanks containing the solution and DMSO.

5.4 Cell culture

Human hepatoma cell line HepG2 were purchased from the Shanghai Institute of Biochemistry and Cell Biology, Chinese Academy of Sciences and cultivated in 1640 medium supplemented with $NaHCO_3$ (2 g/L), fetal bovine serum (10%, v/v), penicillin (100 kU/L) and streptomycin(100 kU/L) at 37 °C in a humidified atmosphere with 95% air and 5% CO_2.

5.5 Cell viability assay

The cytotoxicity was measured by the MTT assay. Briefly, HepG2 cells ((5×10^3 cells/well) were seeded in 96-well plates and cultured for 24 h, treated with indicated concentrations of test compounds for 24 h, followed by its removal and incubation with 900 μM *t*-BHP for another 6 h at 37 °C. Then a solution of MTT (0.5 mg/mL) in

525 fresh medium was added to each well and incubated in a CO_2 incubator for further 4 h.
526 DMSO (100 μL) was added to dissolve formazan crystals, and the absorbance was
527 analyzed in a multiwall-plate reader (Bio-Rad M680) at 570 nm. In the case of inhibi-
528 tion, the cells were pretreated with TRG (100 nM), ZnPP (3 μM), BSO (10 μM),
529 LY294002 (15 μM), DTT (400 μM), SP600125 (25 μM), LY294002 (15μM), NEO
530 (100 nM), DFO (100 μM) or EDTA (500 μM) for 1 h before the addition of the test
531 compounds.

532 *5.6 Measurement for the intracellular ROS levels*

533 HepG2 cells (4×10^5 cells/well) were incubated with the test compounds (1.25, 2.5
534 or 5 μM) or control (DMSO) for 24 h followed by exposing cells to 900μM *t*-BHP for
535 3 h. Then the cells were collected, stained with DCFHA-DA (3 μM) for 30 min at
536 37 °C in the dark, and washed with PBS. The relative fluorescent intensities of FITC
537 were analyzed immediately using a FACSCanto flow cytometer (Becton-Dickinson,
538 San Jose, CA, USA). ROS levels of treatment groups were normalized to the relative
539 control group.

540 *5.7 Western Blot Analysis*

541 HepG2 cells (2×10^6 cells/well) were treated with the test compounds for the indi-
542 cated concentrations and time points, the total protein was lysed and collected by us-
543 ing Cell lysis buffer. Nuclear and cytoplasmic protein extracts were prepared using a
544 Nuclear and Cytoplasmic Protein Extraction Kit (Viagene Biotech, Zhejiang, China)
545 according to the manufacturer's protocol. Concentrations of sample proteins were de-

546 tected by BCA protein assay kit. For western blot analysis, equal amounts (40 μg/lane)
547 of proteins were resolved by 12% SDS-PAGE and electroblotted onto nitrocellulose
548 membranes (Bio-Rad, Hercules, CA) at 4 °C. The membranes were blocked with 5%
549 defatted milk for 1 h at room temperature, washed, and incubated with appropriate
550 specific antibody at 4 °C overnight followed by incubation with the corresponding
551 horseradish peroxidase conjugated secondary antibodies (1/5000) in TBST for another
552 1 h at room temperature. After washing, the protein bands were detected with an en-
553 hanced chemiluminescence (ECL) Western blot detection kit using an enhanced Im-
554 ageQuant chemiluminescence system. In the case of inhibition, the cells were pre-
555 treated with LY294002 (15 μM), SP600125 (25 μM), DTT (400 μM) and CHX (5
556 μg/mL) for 1 h before the addition of the test compounds.

557 *5.8 Assay for Nrf2 half-life*

558 To measure the half-life of Nrf2, the cells were pretreated with or without 5 μM
559 compound **3** for 3 h, followed by treatment with 5 μg/mL CHX (a protein synthesis
560 inhibitor) for the indicated periods. Total cell lysates were collected and subjected to
561 Western blot analysis with an Nrf2 antibody. The densitometric intensity of total Nrf2
562 acquired by blots was performed by using the Image J software (NIH, Bethesda, MD)
563 and plotted against the CHX treatment time to calculate the half-life of Nrf2 [19].

564 *5.9 Statistical analysis*

565 Data are expressed as the mean ± SD. Statistical comparisons among the results
566 were performed using analysis of variance. Significant differences ($P < 0.05$) between

567 the means of two groups were analyzed by Student's *t* test.

568

569 **Acknowledgements**

570 This work was supported by the National Natural Science Foundation of China (Grant

571 Nos. 21372109 and 31100607), and Gansu key technologies R & D program

572 (143NKDA028).

573 **Conflict of Interest**

574 The authors declare no conflict of interest.

575

576 **Appendix A. Supplementary data**

577 Supplementary data associated with this article can be found, in the online version, at

578

ACCEPTED MANUSCRIPT

ACCEPTED MANUSCRIPT

579 **References**

580 [1] W. Jeong, M. Jun, A. Kong, Nrf2: a potential molecular target for cancer chemo-
581 prevention by natural compounds, Antioxid. Redox Signal. 8 (2006) 99-106.

582 [2] K. Itoh, N. Wakabayashi, Y. Katoh, T. Ishii, K. Igarashi, J. Engel, M. Yamamoto,
583 Keap1 represses nuclear activation of antioxidant responsive elements by Nrf2
584 through binding to the amino-terminal Neh2 domain, Genes Dev. 13 (1999) 76-86.

585 [3] N.F. Villeneuve, W. Tian, T. Wu, Z. Sun, A. Lau, E. Chapman, D. Fang, D.D.
586 Zhang, USP15 negatively regulates Nrf2 through deubiquitination of Keap1, Mol.
587 Cell 51 (2013) 68-79.

588 [4] S. Magesh, Y. Chen, L. Hu, Small molecule modulators of Keap1-Nrf2-ARE
589 pathway as potential preventive and therapeutic agents, Med. Res. Rev. 32 (2012)
590 687-726.

591 [5] P. Yao, A. Nussler, L. Liu, L. Hao, F. Song, A. Schirmeier, N. Nussler, Quercetin
592 protects human hepatocytes from ethanol-derived oxidative stress by inducing heme
593 oxygenase-1 via the MAPK/Nrf2 pathways, J. Hepatol. 47 (2007) 253-261.

594 [6] M.K. Kwak, N. Wakabayashi, T.W. Kensler, Chemoprevention through the
595 Keap1-Nrf2 signaling pathway by phase 2 enzyme inducers, Mutat. Res. 555 (2004)
596 133-148.

597 [7] H. Kumar, I.S. Kim, S.V. More, B.W. Kim, D.K. Choi, Natural product-derived
598 pharmacological modulators of Nrf2/ARE pathway for chronic diseases, Nat. Prod.
599 Rep. 31 (2014) 109-139.

600 [8] H.P.T. Ammon, M.A. Wahi, Pharmacology of curcuma longa, Planta Med. 57
601 (1991) 1-7.
602 [9] K. Bairwa, J. Grover, M. Kania, S.M. Jachak, Recent developments in chemistry
603 and biology of curcumin analogues, RSC Adv. 4 (2014) 13946.
604 [10] M.A. Tomren, M. Masson, T. Loftsson, H.H. Tonnesen, Studies on curcumin and
605 curcuminoids XXXI. Symmetric and asymmetric curcuminoids: stability, activity and
606 complexation with cyclodextrin, Int. J. Pharm. 338 (2007) 27-34.
607 [11] S.V. Jovanovic, C.W. Boone, S. Steenken, M. Trinoga, R.B. Kaskey., How cur-
608 cumin works preferentially with water soluble antioxidants, J. Am. Chem. Soc. 123
609 (2001) 3064-3068.
610 [12] A.T. Dinkova-Kostova, M.A. Massiah, R.E. Bozak, R.J. Hicks, P. Talalay, Po-
611 tency of Michael reaction acceptors as inducers of enzymes that protect against car-
612 cinogenesis depends on their reactivity with sulfhydryl groups, Proc. Natl. Acad. Sci.
613 U. S. A. 98 (2001) 3404-3409.
614 [13] E. Balogun, M. Hoque, P. Gong, E. Killeen, C.J. Green, R. Foresti, J. Alam, R.
615 Motterlini, Curcumin activates the haem oxygenase-1 gene via regulation of Nrf2 and
616 the antioxidant-responsive element, Biochem. J. 371 (2003) 887-895.
617 [14] S. Prasad, S.C. Gupta, A.K. Tyagi, B.B. Aggarwal, Curcumin, a component of
618 golden spice: from bedside to bench and back, Biotechnol. Adv. 32 (2014) 1053-1064.
619 [15] T. Esatbeyoglu, P. Huebbe, I.M. Ernst, D. Chin, A.E. Wagner, G. Rimbach, Cur-
620 cumin-from molecule to biological function, Angew. Chem. Int. Ed. 51 (2012)

621 5308-5332.

622 [16] Y.M. Han, D.S. Shin, Y.J. Lee, I.A. Ismail, S.H. Hong, D.C. Han, B.M. Kwon,
623 2-Hydroxycurcuminoid induces apoptosis of human tumor cells through the reactive
624 oxygen species-mitochondria pathway, Bioorg. Med. Chem. Lett. 21 (2011) 747-751.

625 [17] S.M. Bayomi, H.A. El-Kashef, M.B. El-Ashmawy, M.N.A. Nasr, M.A.
626 El-Sherbeny, F.A. Badria, L.A. Abou-zeid, M.A. Ghaly, N.I. Abdel-Aziz, Synthesis
627 and biological evaluation of new curcumin derivatives as antioxidant and antitumor
628 agents, Med. Chem. Res. 22 (2012) 1147-1162.

629 [18] H. Endo, Y. Nikaido, M. Nakadate, S. Ise, H. Konno, Structure activity relation-
630 ship study of curcumin analogues toward the amyloid-beta aggregation inhibitor,
631 Bioorg. Med. Chem. Lett. 24 (2014) 5621-5626.

632 [19] D. Lin, F. Dai, L.D. Sun, B. Zhou, Toward an understanding of the role of a cat-
633 echol moiety in cancer chemoprevention: The case of copper- and
634 o-quinone-dependent Nrf2 activation by a catechol-type resveratrol analog, Mol. Nutr.
635 Food Res. 59 (2015) 2395-2406.

636 [20] U. Pedersen, P.B. Rasmussen, S.O. Lawesson, Synthesis of naturally occurring
637 curcuminoids and related compounds, Eur. J. Org. Chem. 1985 (1985) 1557-1569.

638 [21] S. Park, A. Kim, M. Lee, Synergic effects of α-tocopherol and β-carotene on
639 tert-butylhydroperoxide-induced HepG2 cell injury, Toxicol. Ind. Health 25 (2009)
640 311–320.

641 [22] C.Y. Chu，T.H. Tseng，J.M. Hwang，F.P. Chou，C.J. Wang, Protective effects of

642 capillarisin on tert-butylhydroperoxide-induced oxidative damage in rat primary
643 hepatocytes, Arch. Toxicol. 73 (1999) 263-268.
644 [23] A. Arlt, S. Sebens, S. Krebs, C. Geismann, M. Grossmann, M.L. Kruse, S.
645 Schreiber, H. Schafer, Inhibition of the Nrf2 transcription factor by the alkaloid
646 trigonelline renders pancreatic cancer cells more susceptible to apoptosis through de-
647 creased proteasomal gene expression and proteasome activity, Oncogene 32 (2013)
648 4825-4835.
649 [24] Y.M.B. Greenwald, S. Anzi, S. Ben Sasson, H. Bianco-Peled, R. Kohen, Can ni-
650 troxides evoke the Keap1-Nrf2-ARE pathway in skin?, Free Radic. Biol. Med. 77
651 (2014) 258-269.
652 [25] D.D. Zhang, Mechanistic studies of the Nrf2-Keap1 signaling pathway, Drug
653 Metab. Rev. 38 (2006) 769-789.
654 [26] T. Nguyen, P. Nioi, C.B. Pickett, The Nrf2-antioxidant response element signal-
655 ing pathway and its activation by oxidative stress, J. Biol. Chem. 284 (2009)
656 13291-13295.
657 [27] Y. Zhu, P. Wang, Y. Zhao, C. Yang, A. Clark, T. Leung, X. Chen, S. Sang, Syn-
658 thesis, evaluation, and metabolism of novel [6]-shogaol derivatives as potent Nrf2 ac-
659 tivators, Free Radic. Biol. Med. 95 (2016) 243-254.
660 [28] A.L. Eggler, G. Liu, J.M. Pezzuto, R.B. van Breemen, A.D. Mesecar, Modifying
661 specific cysteines of the electrophile-sensing human Keap1 protein is insufficient to
662 disrupt binding to the Nrf2 domain Neh2, Proc. Natl. Acad. Sci. U. S. A. 102 (2005)

663 10070-10075.

664 [29] I. Almazari, J.M. Park, S.A. Park, J.Y. Suh, H.K. Na, Y.N. Cha, Y.J. Surh, Gug-
665 gulsterone induces heme oxygenase-1 expression through activation of Nrf2 in human
666 mammary epithelial cells: PTEN as a putative target, Carcinogenesis 33 (2012)
667 368-376.

668 [30] S. Li, J. Li, C. Shen, X. Zhang, S. Sun, M. Cho, C. Sun, Z. Song,
669 tert-Butylhydroquinone (tBHQ) protects hepatocytes against lipotoxicity via inducing
670 autophagy independently of Nrf2 activation, Biochim. Biophys. Acta. 1841 (2014)
671 22-33.

672 [31] L.J. Deny, H. Traboulsi, A.M. Cantin, E. Marsault, M.V. Richter, G. Belanger,
673 Bis-Michael acceptors as novel probes to study the Keap1/Nrf2/ARE pathway, J. Med.
674 Chem. 59 (2016) 9431-9442.

675 [32] E.J. Smith, K.P. Shay, N.O. Thomas, J.A. Butler, L.F. Finlay, T.M. Hagen,
676 Age-related loss of hepatic Nrf2 protein homeostasis: Potential role for heightened
677 expression of miR-146a, Free Radic. Biol. Med. 89 (2015) 1184-1191.

678 [33] X.J. Wang, J.D. Hayes, L.G. Higgins, C.R. Wolf, A.T. Dinkova-Kostova, Activa-
679 tion of the NRF2 signaling pathway by copper-mediated redox cycling of para- and
680 ortho-hydroquinones, Chem. Biol. 17 (2010) 75-85.

681 [34] F. Tisato, C. Marzano, M. Porchia, M. Pellei, C. Santini, Copper in diseases and
682 treatments, and copper-based anticancer strategies, Med. Res. Rev. 30 (2010)
683 708-749.

684 [35] L.M. Bystrom, S. Rivella, Cancer cells with irons in the fire, Free Radic. Biol.
685 Med. 79 (2015) 337-342.
686 [36] Y. Nakamura, N. Miyoshi, Electrophiles in foods: the current status of isothiocy-
687 anates and their chemical biology, Biosci. Biotechnol. Biochem. 74 (2010) 242-255.
688 [37] S.A. Lipton, T. Rezaie, A. Nutter, K.M. Lopez, J. Parker, K. Kosaka, T. Satoh,
689 S.R. McKercher, E. Masliah, N. Nakanishi, Therapeutic advantage of
690 pro-electrophilic drugs to activate the Nrf2/ARE pathway in Alzheimer's disease
691 models, Cell Death. Dis. 7 (2016) e2499.
692 [38] T. Satoh, S.R. McKercher, S.A. Lipton, Nrf2/ARE-mediated antioxidant actions
693 of pro-electrophilic drugs, Free Radic. Biol. Med. 65 (2013) 645-657.
694 [39] G Scapagnini, R Foresti, V Calabrese, AM Giuffrida Stella, CJ Green, R Motter-
695 lini, Caffeic acid phenethyl ester and curcumin: a novel class of heme oxygenase-1
696 inducers, Mol. Pharmacol. 3 (2002) 554–561.
697 [40] L. Mira, M. Tereza Fernandez, M. Santos, R. Rocha, M. Helena Florêncio, K.R.
698 Jennings, Interactions of flavonoids with iron and copper ions: a mechanism for their
699 antioxidant activity, Free Radic. Res. 36 (2009) 1199-1208.
700 [41] G.Y. Kreitman, J.C. Danilewicz, D.W. Jeffery, R.J. Elias, Reaction mechanisms
701 of metals with hydrogen sulfide and thiols in model wine. Part 1: copper-catalyzed
702 oxidation, J. Agric. Food Chem. 64 (2016) 4095-4104.
703 [42] G.Y. Kreitman, J.C. Danilewicz, D.W. Jeffery, R.J. Elias, Reaction mechanisms
704 of metals with hydrogen sulfide and thiols in model wine. Part 2: iron- and cop-

705 per-catalyzed oxidation, J. Agric. Food Chem. 64 (2016) 4105-4113.

706 [43] M. ópezlázaro, Anticancer and carcinogenic properties of curcumin: Considera-

707 tions for its clinical evelopment as a cancer chemopreventive and hemotherapeutic

708 agent, Mol. Nutr. Food Res. 52 (2008) 103-127.

709 [44] L.A. Adams, V.K. Aggarwal, R.V. Bonnert, B. Bressel, R.J. Cox, J. Shepherd, J.d.

710 Vicente, M. Walter, W.G. Whittingham, C.L. Winn, Diastereoselective synthesis of

711 cyclopropane amino acids using diazo compounds generated in situ, J. Org. Chem. 68

712 (2003) 9433-9440.

713 [45] D.P. Flaherty, T. Kiyota, Y. Dong, T. Ikezu, J.L. Vennerstrom, Phenolic

714 bis-styrylbenzenes as beta-amyloid binding ligands and free radical scavengers, J.

715 Med. Chem. 53 (2010) 7992-7999.

716 [46] F. Dai, G.Y. Liu, Y. Li, W.J. Yan, Q. Wang, J. Yang, D.L. Lu, D.J. Ding, D. Lin, B.

717 Zhou, Insights into the importance for designing curcumin-inspired anticancer agents

718 by a prooxidant strategy: The case of diarylpentanoids, Free Radic. Biol. Med. 85

719 (2015) 127-137.

720

ACCEPTED MANUSCRIPT

721 Lists of Captions:
722

723 **Figure 1:** Molecular structures of curcumin and its designed analogs.

724

725 **Figure 2:** Stability of curcumin and its selected analogs (40 μM) in PBS (pH 7.4)
726 were assessed by monitoring their UV-visible absorption changes (interval = 2 min) at
727 25 °C for 30 min.

728

729 **Figure 3:** Cytotoxicity (A) and cytoprotection (B) of curcumin and its analogs against
730 the *t*-BHP-induced HepG2 cell death. (A) Cytotoxicity of curcumin and its analogs (5
731 μM) towards HepG2 cells (5×10^3 cells/well) for 24 h, and cell viability was meas-
732 ured by the MTT assay. (B) HepG2 cells were pretreated with the curcumin and its
733 analogs (5 μM) for 24 h, followed by their removal and incubation with 900 μM
734 *t*-BHP for another 6 h. All data represent the mean ± SD of three independent experi-
735 ments. **p < 0.01 of *t*-BHP-treated group versus the vehicle group; #p < 0.05 and ##p
736 < 0.01 versus the t-BHP-treated group.

737

738 **Figure 4:** Compound **3** alleviates the *t*-BHP-induced oxidative death (A) and ROS
739 accumulation (B) in a dose-dependent manner. **p < 0.01 of *t*-BHP control group
740 versus the vehicle group; #p < 0.05 and ##p < 0.01 versus the *t*-BHP-stimulated
741 group.

742

743 **Figure 5:** Compound **3** triggers Nrf2 activation and its downstream gene expression.

744 Time- (A) and dose-dependent (B) promotion of Nrf2 nuclear translocation by com-
745 pound **3**. Time- (C) and dose-dependent (D) increases in the protein expression of
746 HO-1, GCLC, and GCLM by compound **3**. A comparison of compound **3** with *t*-BHQ
747 in the cytoprotection (E) and Nrf2 activation (F) and its downstream gene expression
748 (G). All data represent the mean ± SD of three independent experiments. **p < 0.01
749 of *t*-BHP-treated group versus the vehicle group; #p < 0.05 and ##p < 0.01 versus the
750 t-BHP-treated group.
751
752 **Figure 6:** Effects of TRG (A), ZnPP (B) and BSO (C) on the cytoprotection induced
753 by compound **3.** **p < 0.01 of *t*-BHP control group versus the vehicle group; #p <
754 0.05 and ##p < 0.01 versus the *t*-BHP-stimulated group.
755
756 **Figure 7:** Compound **3** activates Nrf2 *via* provoking phosphorylation of Akt and JNK.
757 (A) Effect of compound **3** on phosphorylation of Akt, JNK and ERK. (B) Effects of
758 LY294002 and SP600125 on the cytoprotection induced by compound **3**. (C) Effects
759 of LY294002 and SP600125 on the expression of Phase II detoxifying enzyme in-
760 duced by compound **3**. **p < 0.01 of *t*-BHP-treated group versus the vehicle group;
761 #p < 0.05 and ##p < 0.01 versus the *t*-BHP-treated group.
762
763 **Figure 8:** Compound **3** triggers Nrf2 activation through disrupting Keap1-Nrf2 com-
764 plex and slowing Nrf2 degradation. (A and B) Immunoblot analysis of the indicated

765 proteins related to cytoprotection in the compound **3**-treated cells at 3 h in the pres-
766 ence or absence of pretreatment with DTT for 1 h. (C) Compound **3** upregulates Nrf2
767 expression in a time-dependent manner. (D and E) Effect of compound **3** on stability
768 of Nrf2. HepG2 cells were pretreated with or without compound **3** (5μM) for 3 h, fol-
769 lowed by co-incubation with CHX (5 μg/mL) for 24 h.

770

771 **Figure 9:** Effects of DTT, NEO, EDTA and DFO on the compound **3**-induced cyto-
772 protection. **p < 0.01 of *t*-BHP-treated group versus the vehicle group; #p < 0.05 and
773 ##p < 0.01 versus the *t*-BHP-treated group.

774

775 **Figure 10:** Proposed mechanisms underlying the cytoprotection of compound **3** in the
776 model of *t*-BHP-induced HepG2 cell death.

ACCEPTED MANUSCRIPT

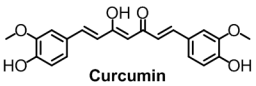
Curcumin

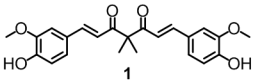
1

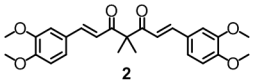
2

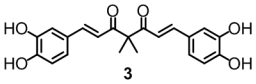
3

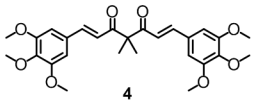
4

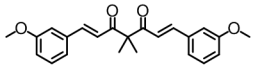
5

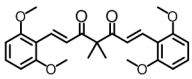
6

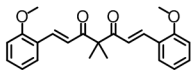
7

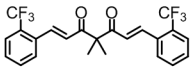
8

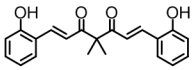
9

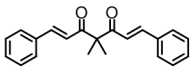
10

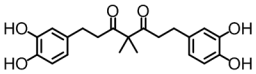
3-H

ACCEPTED MANUSCRIPT

A

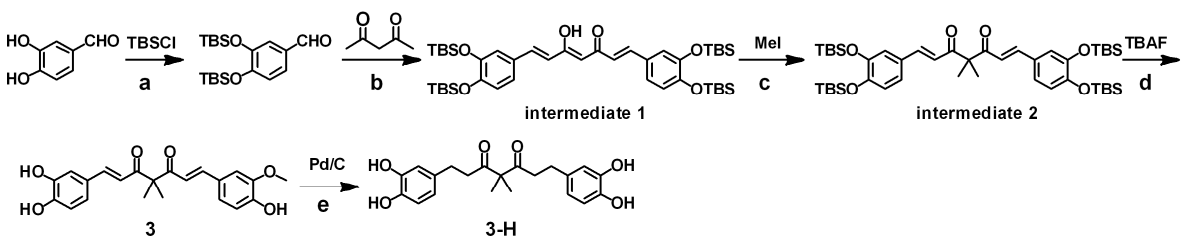

B

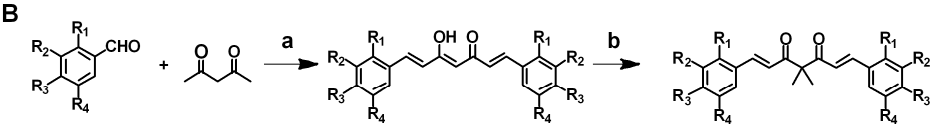

2: $R_2 = R_3 = OMe$, $R_1 = R_4 = R_5 = H$
4: $R_2 = R_3 = R_4 = OMe$, $R_1 = R_5 = H$
5: $R_2 = OMe$, $R_1 = R_3 = R_4 = R_5 = H$
6: $R_3 = OMe$, $R_1 = R_2 = R_4 = R_5 = H$
7: $R_1 = OMe$, $R_2 = R_3 = R_4 = R_5 = H$
8: $R_1 = CF_3$, $R_2 = R_3 = R_4 = R_5 = H$
10: $R_1 = R_2 = R_3 = R_4 = R_5 = H$
11: $R_2 = R_3 = OMe$, $R_1 = R_4 = R_5 = H$

C

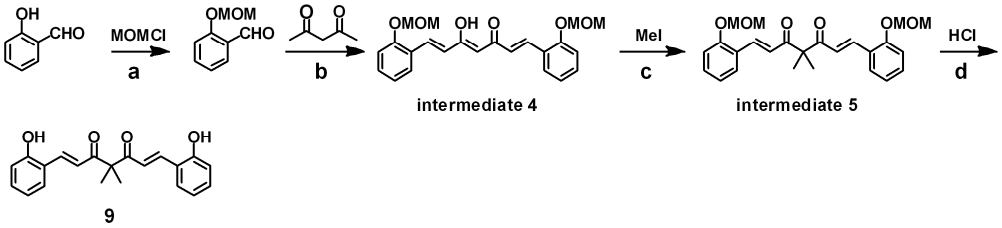

ACCEPTED MANUSCRIPT

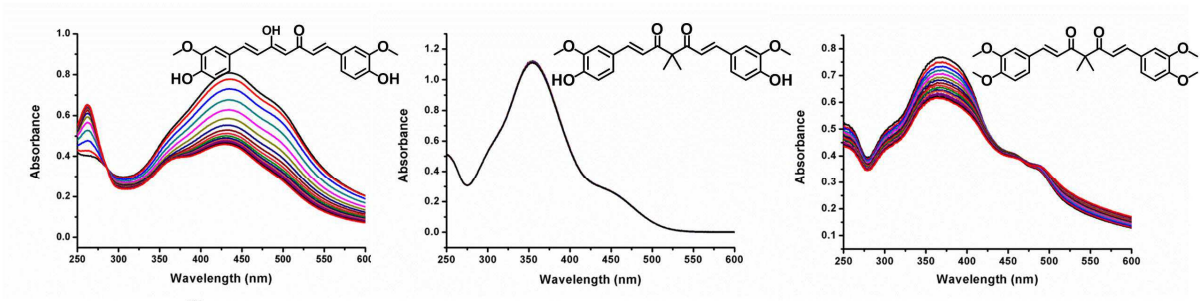

Cur 1 2

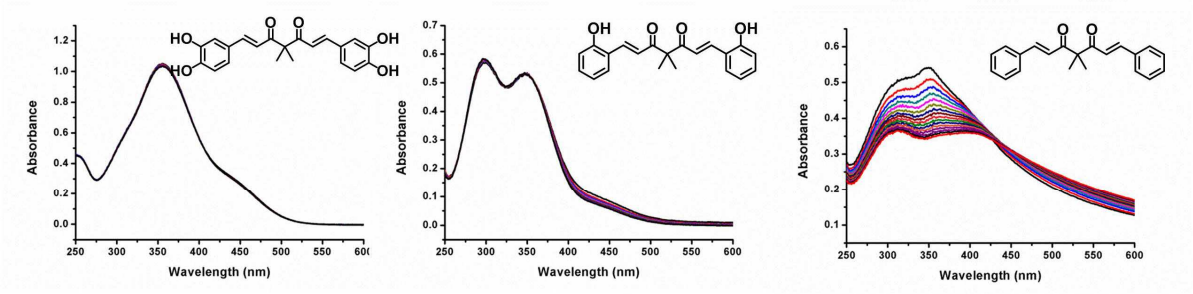

3 9 10

ACCEPTED MANUSCRIPT

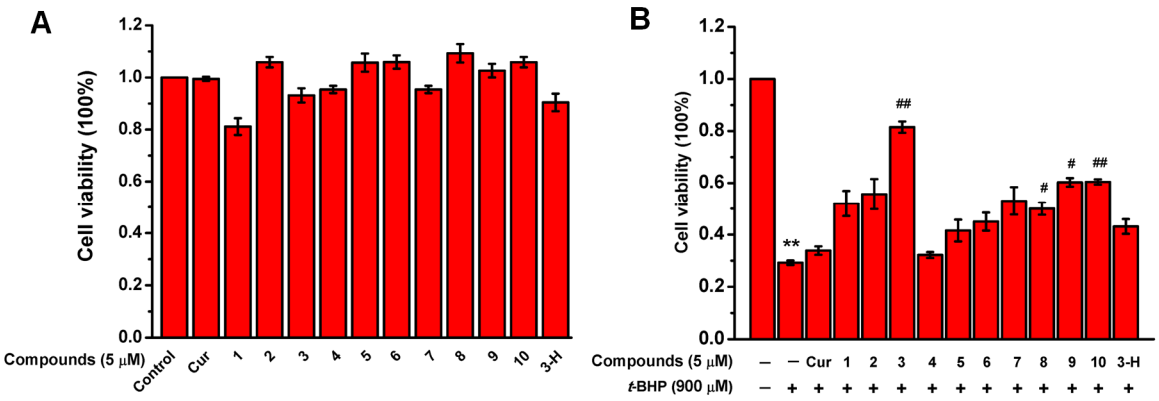

ACCEPTED MANUSCRIPT

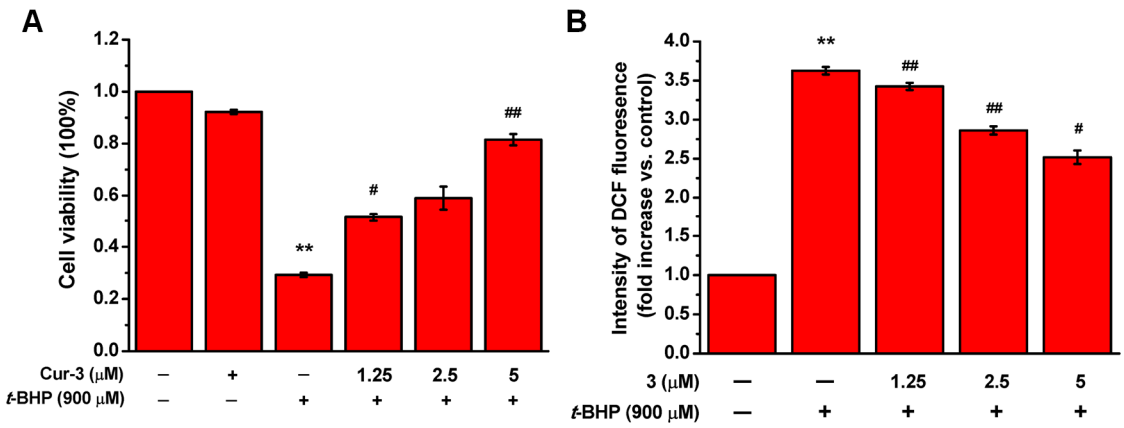

ACCEPTED MANUSCRIPT

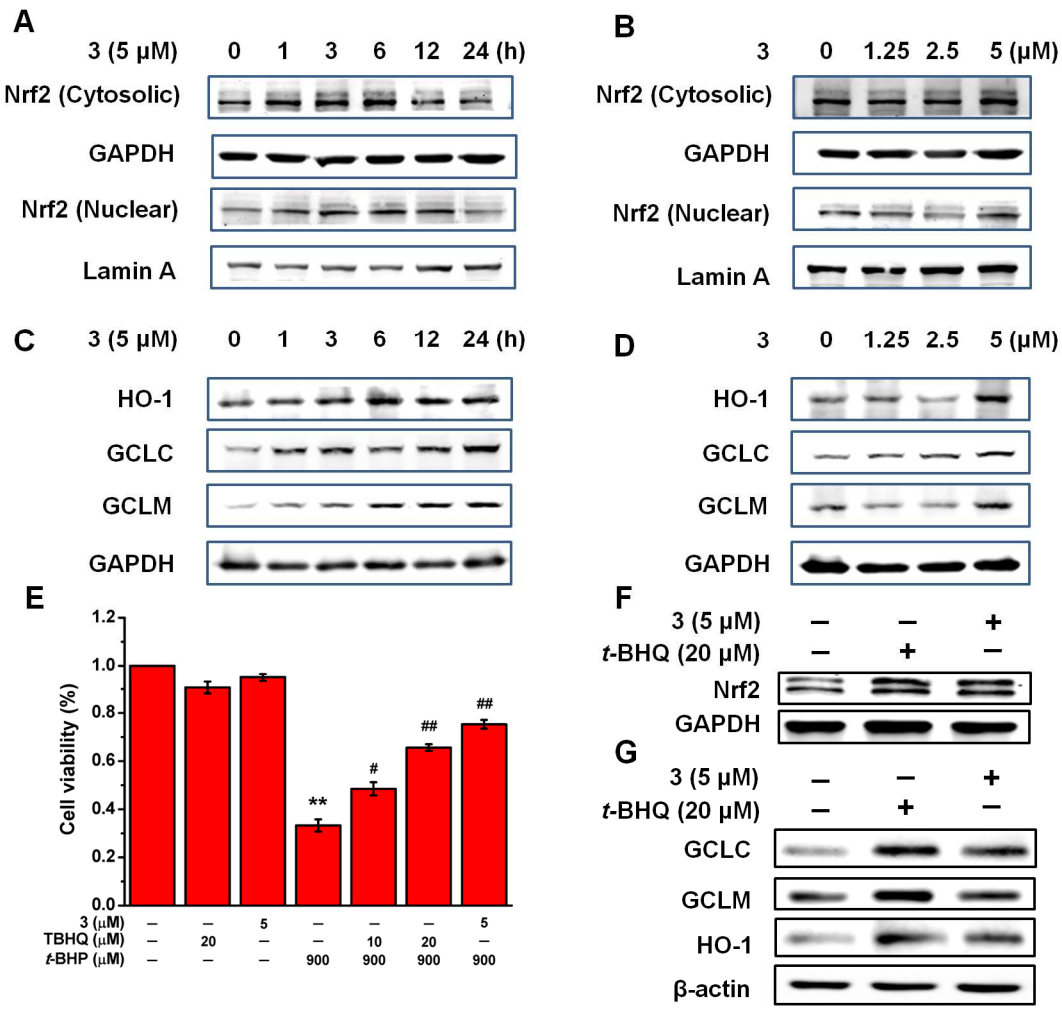

ACCEPTED MANUSCRIPT

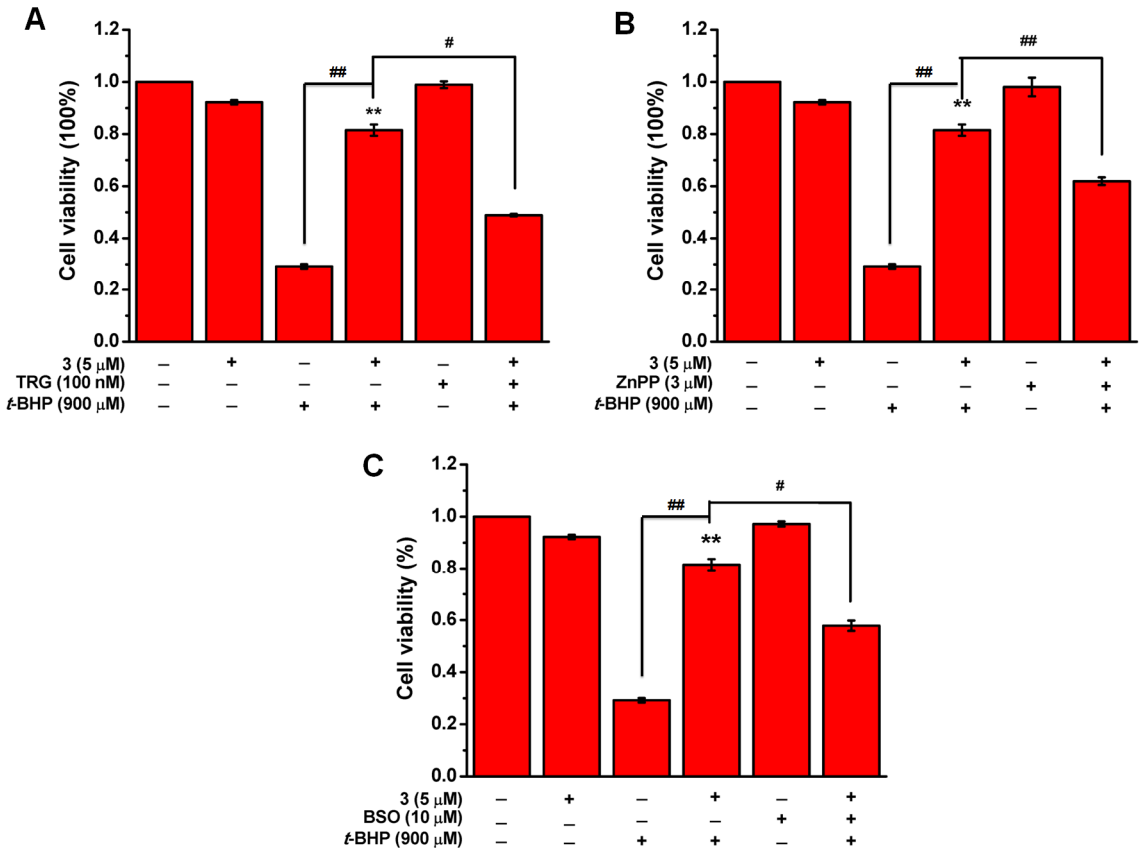

ACCEPTED MANUSCRIPT

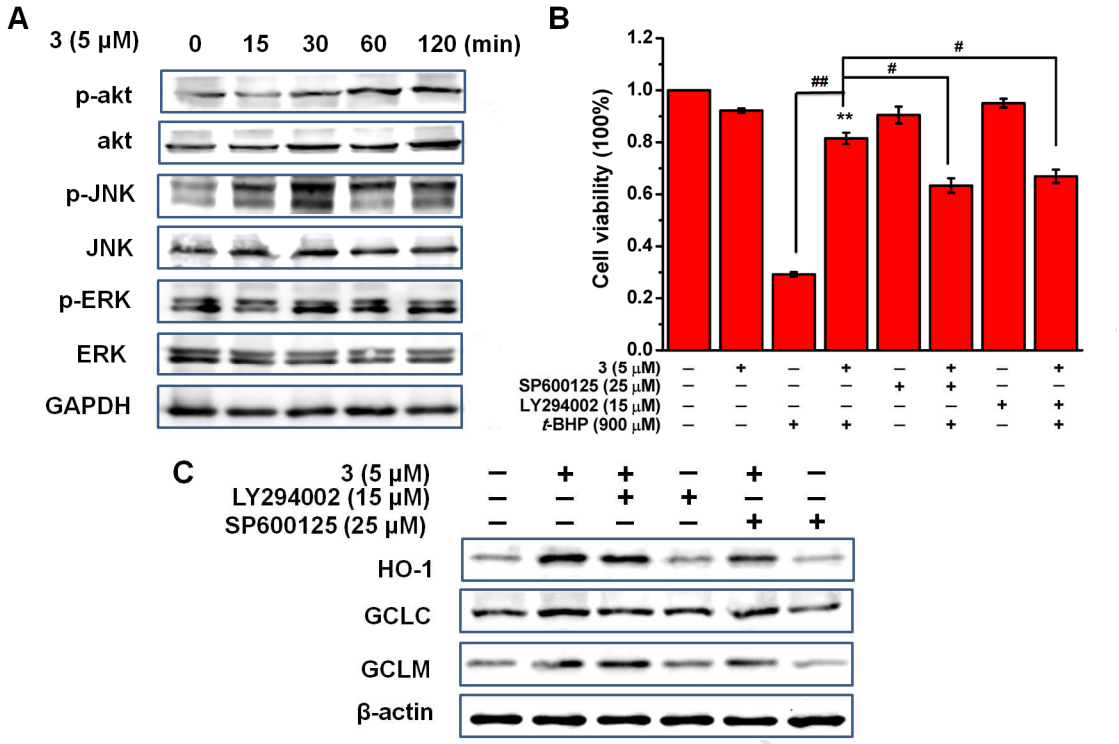

ACCEPTED MANUSCRIPT

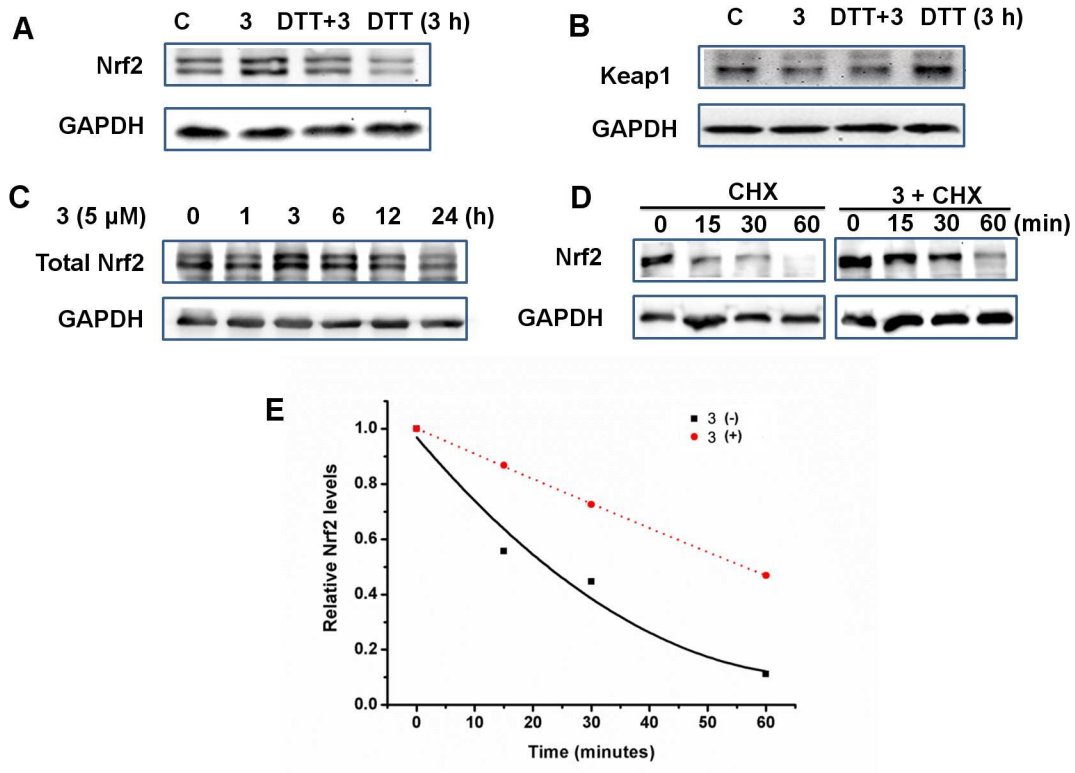

ACCEPTED MANUSCRIPT

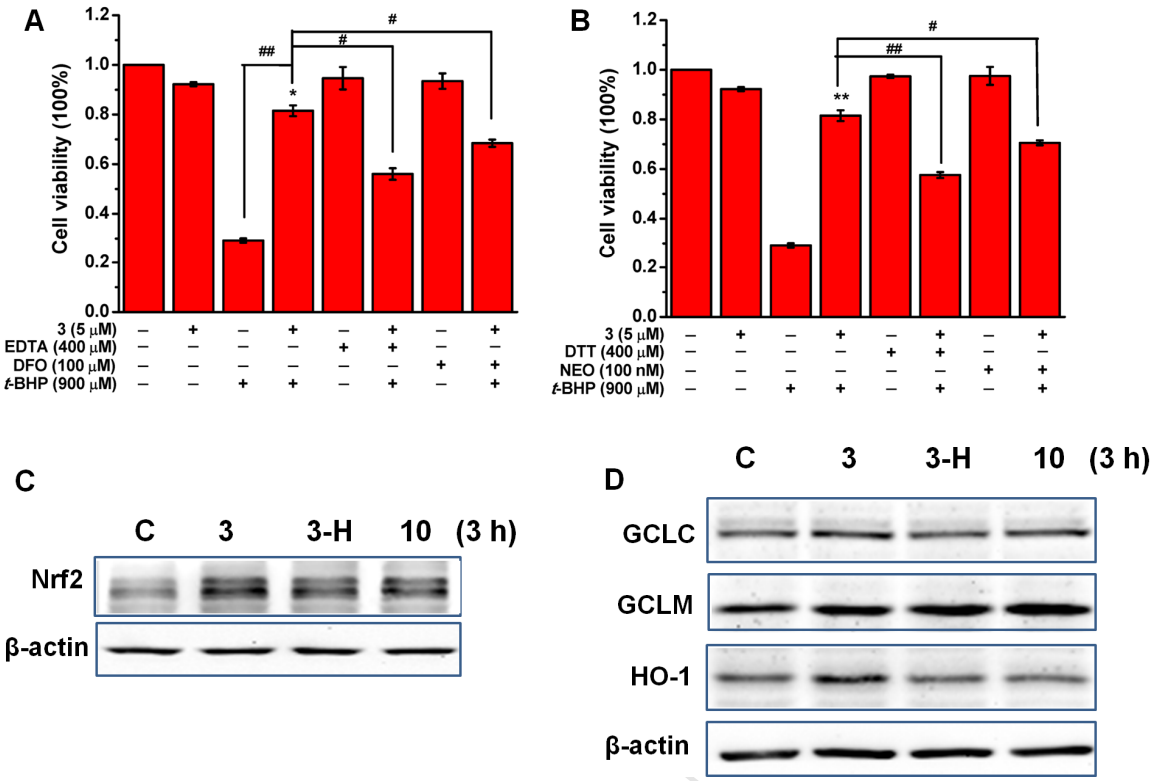

ACCEPTED MANUSCRIPT

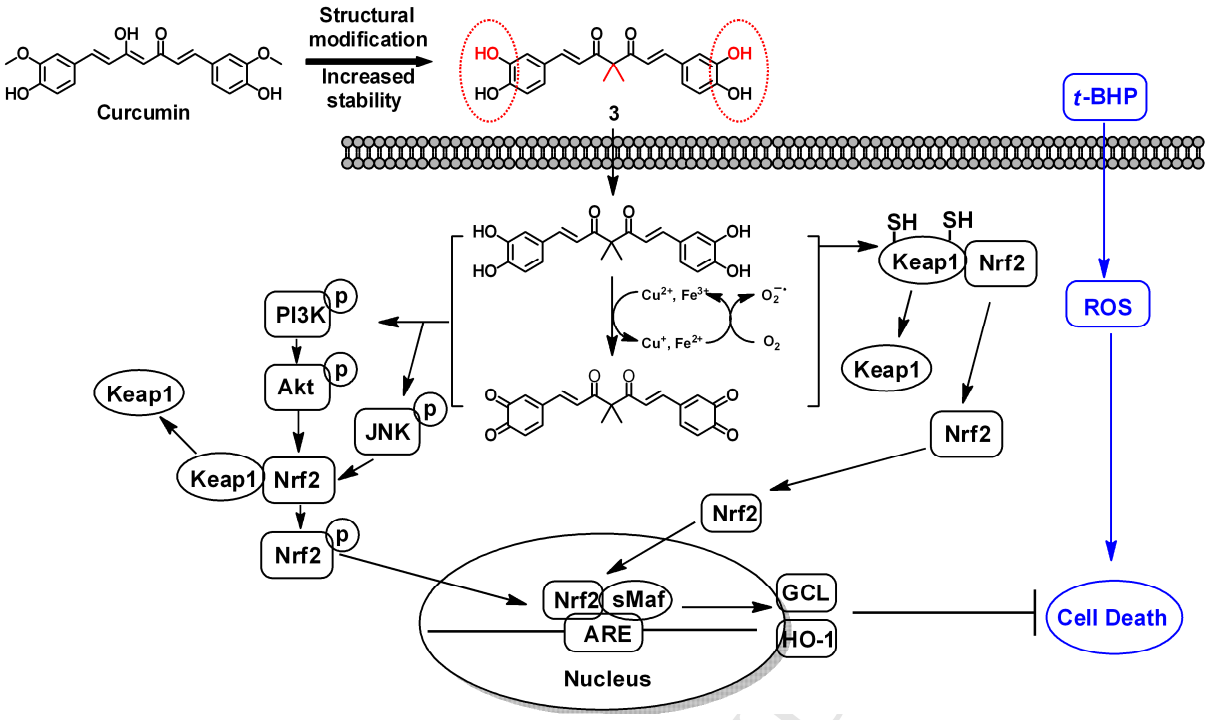

ACCEPTED MANUSCRIPT

ACCEPTED MANUSCRIPT

Research highlights

- New curcumin-inspired Nrf2 activators and cytoprotectors were designed
- The design was based on a stability-increasing and proelectrophilic strategy
- A geminally dimethylated and catechol-type curcumin analog surfaced as a lead
- Nrf2-dependent cytoprotection is Michael acceptor- and catechol-dependent
- Copper and iron-mediated oxidation of catechol is required for the cytoprotection

ACCEPTED MANUSCRIPT